Monitoring of Offshore Platform Deformation with Stanford Method of Persistent Scatterer (StaMPS)

Amir Sharifuddin Ab Latip
Civil and Environmental Engineering Department,
Universiti Teknologi PETRONAS,
Perak, Malaysia.
asharifuddin2@gmail.com

Anuphao Aobpaet
Geo-Informatics and Space Technology
Development Agency,
Chonburi, Thailand.
anuphao@gistda.or.th

Abd Nasir Matori
Civil and Environmental Engineering Department,
Universiti Teknologi PETRONAS,
Perak, Malaysia.
nasrat@petronas.com.my

Ami Hassan Md Din
Department of Geoinformation,
Faculty of Geoinformation and Real Estate,
Universiti Teknologi Malaysia,
Johor Bahru, Malaysia
amihassanmddin@gmail.com

Abstract— Numerous studies have proven that the Persistent Scatterer Interferometry (PSI) techniques have been successfully utilized for land subsidence monitoring, slope stability monitoring, volcano deformation, earthquake deformation, urban deformation and dike monitoring. However, the ability of PSI technique for the application of the offshore structures such as offshore oil platform has been less recognized. With the PSI techniques, the deformation information can be extracted from solid or man-made features of offshore structures which have higher radar backscatter features. Therefore, this paper investigates the capabilities of PSI technique using Stanford Method of Persistent Scatterer (StaMPS) for monitoring deformation phenomena of an offshore platform. A total number of 11 high resolution X-band data from TerraSAR-X radar images covering the period from 2012 to 2013 are utilized to apply the StaMPS method. The results show deformation rate of the offshore platform is in the range between -6 mm/year and 8.1 mm/year and its standard deviation from 0.8 to 3.1 mm/year which is comparable to deformation monitoring result from Global Positioning System (GPS) technique done earlier. Therefore it shows the potential of using PSI technique for such deformation monitoring of an offshore structure.

Keywords— offshore platform; deformation; StaMPS method

I. INTRODUCTION

Reservoir compaction or shallow gas phenomena may cause offshore platforms to experience deformation which could affect their structural integrity. Excessive deformation may also cause loss of production, affect the efficiency of the machinery on board the platform as well as loss of live. Hence it is very crucial to monitor the deformation of offshore platform against occurrences of serious deformation. The physical location of many offshore platforms which are typically hundreds of kilometers offshore merits the use of satellite-based Interferometric Synthetic Aperture Radar (InSAR) technique to perform the monitoring. The technique also provides a chance to frequently monitor the offshore platform without the needs for personnel intrusion to the offshore structures, which more often than not poses logistical challenge.

Synthetic Aperture Radar (SAR) is a radar imaging system that transmits signals of microwave through a space-borne SAR instrument (SAR antenna) on board of a satellite in this case to illuminate targets in the surface. The backscattered signals that are received on the SAR antenna represent the characteristics of the targets. Also, two types of information are recorded from the backscattered signals which are the amplitude and phase of the SAR signal. The phase represents the travelling of the signal from its emission to its return, whereas the amplitude represents the backscattering capability of the surface sending the incident energy back to the antenna. By precisely measuring the time difference between the transmission and reception of the signal, the distance between radar antenna and the target can be determined and known as slant range. Temporal changes of the target can be determined by combining multiple SAR images acquired over the same area at different moment of times. If the target on the surface remains static as for stable surface, the distance between radar antenna and target will remain constant. Otherwise it would indicate moving target which indicates some kind of surface movement.

The method to identify the persistent scatterers was first proposed by [1] and called as Permanent Scatterer Interferometric Synthetic Aperture Radar (PSInSAR). This method utilizes amplitude analysis in a series of interferograms to identify the persistent scatterers. This method is more successful in urban areas where man-made structures have higher reflectivity. The deformation is then estimated based on the similarity of their phase history to an approximate model (e.g., linear or periodic) of how deformation varies through time. Later, [2] developed a new method called Stanford Method for Persistent Scatterer (StaMPS). This method utilizes a combination of amplitude and phase analysis to identify the persistent scatterers, which has proven to be reliable even in natural terrains. The

This work was supported by the Fundamental Research Grant Scheme (FRGS) from the Ministry of Higher Education (Malaysia) [grant number: 0153AB-I59].

method utilizes the spatial correlation of the phases instead of a defined phase history thus the temporal variation of deformation can be observed. This method substantially provides reliable deformation measurements in irregular deformation areas.

In this study, the StaMPS method is briefly explained and utilized to understand the spatial and temporal characteristics of offshore platform deformation. The SAR images from TerraSAR-X satellite are collected over the study area, during the time period of 2012 to 2013. The surface deformation rate in mm per year along the line of sight (LOS) direction of satellite is obtained.

II. METHODOLOGY

A. Study area

In this study, one of the PETRONAS offshore platforms called as P platform is utilized as monitored platform (see Fig. 1). The P platform is situated approximately 250 km off the east coast of Peninsular Malaysia at a water depth of 77 m. The dimension of the P platform is 30.73 m (width) by 58.81 m (length). The P platform is a fixed platform which has facilities to drill wells and temporarily store the oil and gas products until they can be transported through pipelines to shore for refining. The P platform is selected as a test site to apply the StaMPS method due to its previous deformation records based on Global Positioning System (GPS) technique revealed the P platform has the deformation rate as much as 0.0094 m within the period of two months [3]. Therefore, the deformation monitoring of the P platform is crucial in order to mitigate hazards of excessive deformation which may lead to structural failure to the structure.

Fig. 1. P platform (Source: [4])

B. Data acquisition

A total number of 11 TerraSAR-X images in the StripMap mode (3 m resolution) are acquired on descending satellite passes from August 2012 to April 2013. One of the images on 04th January 2013 is selected as master image after considering the baseline lengths and time spans. The maximum distribution of spatial perpendicular baselines and temporal baselines with respect to a single master image are 350 m and 132 days, respectively. Table I shows the date of the images acquisition, perpendicular (B_{perp}) and temporal (B_{temp}) baselines with respect to the master image.

TABLEI. Image number, date of acquisition, perpendicular baseline length and temporal baseline with respect to the master image.

Image number	Date (dd/mm/yyyy)	Perpendicular baseline (B_{perp}) [meters]	Temporal Baseline (B_{temp}) [days]
1	25.08.2012	173	132
2	27.09.2012	185	99
3	30.10.2012	-350	66
4	21.11.2012	-77	44
5	13.12.2012	186	22
6	24.12.2012	-40	11
7	**04.01.2013**	**0**	**0**
8	26.01.2013	31	22
9	17.02.2013	-23	44
10	22.03.2013	276	77
11	24.04.2013	-67	110

C. StaMPS Method

The procedures of PSI processing using StaMPS method as shown in Fig. 2 can be divided into four main parts, which are interferograms formation, phase stability estimation, PS selection and deformation estimation.

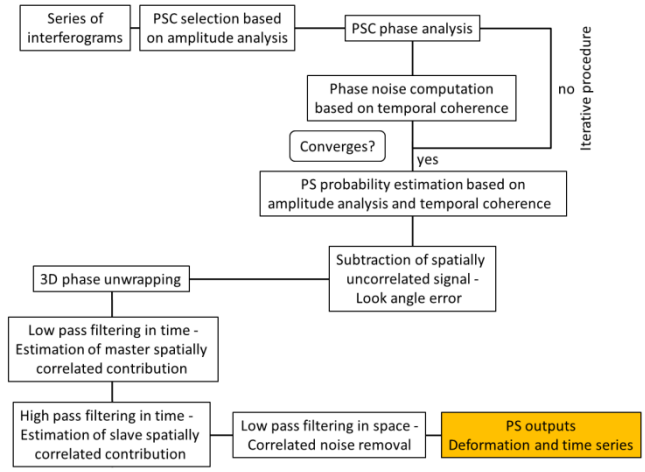

Fig. 2. Flow chart PSI processing in StaMPS method. (Modified from [5])

The processing begins by reading SAR images (i.e., in the Single Look Complex format). There are three considerations in selecting a master image from the total of available SAR images (i.e., perpendicular baseline, temporal baseline and doppler centroid frequency). The perpendicular baselines and temporal baselines should be distributed as short as possible and the doppler centroid frequency difference near the average doppler centroid in order to maximises the correlation sum of all utilized interferograms. The SAR images are cropped to the area around the P platform to minimize the co-registration error that might be

occurred since the area is surrounded by ocean. The ocean is smooth surface and constantly moving, the backscattering are decreased making the amplitude of each pixel become low and appear as dark pixel in the SAR images. The co-registration of SAR images is important for the interferogram generation. The purpose of the co-registration is to align the SAR images in the same geometry for determining the phase difference of the same area. The co-registered images are then processed to generate interferogram. The interferogram is formed by differencing the phase of all slave images to the phase of the master image. For N+1 SAR images, N inteferograms can be generated with respect to the master image. The interferometric phase has generally appeared as a series of fringes. Each fringe in the interferogram represents one full colour cycle changing from red to green to blue.

The persistent scatterer candidates (PSC) are dominated scatterers in a series of interferograms based on the pixels that exhibit the amplitude stability over time which is defined by [6] as:

$$D_A = \frac{\sigma_a}{\mu_a} \tag{1}$$

where D_A is the amplitude dispersion index, σ_a is the standard deviation of the amplitude return relative to each individual pixel and μ_a is its average. The amplitude dispersion index is useful to reduce the initial number of pixels for phase analysis. However, the higher threshold value of 0.4 is utilized compared to 0.25 that was suggested by [6] for the amplitude dispersion index because the phase analysis of the selected PSC points in the next step does not require that most PSC are being PS.

For a PSC (x) in the *i-th* topographically corrected interferogram, the interferometric phase $\phi_{\text{int}x,i}$ can be written as [7]:

$$\phi_{\text{int}x,i} = W\left\{\phi_{def,x,i} + \phi_{a,x,i} + \phi_{orb,x,i} + \phi_{\varepsilon,x,i} + n_{x,i}\right\} \tag{2}$$

where the right side contains phase contribution from surface deformation ϕ_{def}, atmospheric delay ϕ_a, orbital error ϕ_{orb}, look angle error ϕ_ε and noise n . W represents the wrapped operator. To analyse the phase stability of the selected PSC, the phase contribution due to the noise should be small enough. However, variations in the first four components in Equation (2) dominate the noise component, making difficult to identify which scatterers are stable. The variations of the first three components are spatially correlated while the fourth component is spatially uncorrelated. Thus, the phase contributions due to the three components are estimated using band pass filtering of surrounding pixels. The look angle error can be estimated through its correlation with the perpendicular baseline.

The temporal coherence γ_x as shown in Equation (3) is calculated to measure the phase noise level after correcting the spatially correlated phase and the look angle error of a PSC pixel and also evaluate whether the pixel is a PS point:

$$\gamma_x = \frac{1}{N}\left|\sum_{i=1}^{N} \exp\left\{j\left(\varphi_{\text{int},x,i} - \overline{\varphi}_{\text{int},x,i} - \Delta\hat{\varphi}_{\varepsilon,x,i}\right)\right\}\right| \tag{3}$$

where N is the number of interferogram, $\overline{\varphi}_{\text{int},x,i}$ is the estimate of the spatially correlated components and $\Delta\hat{\varphi}_{\varepsilon,x,i}$ is the estimate of the look angle error. The PS points are selected based on pixels have higher γ_x values. Thus, the pixels have lower γ_x are rejected. All the fourth components are again estimated for the remaining PSC pixels. The γ_x is then calculated for every PSC. Generally, the values of noise component will decrease and converge after a few iterations thus the γ_x is dominated by the small noise.

The PS probability is estimated for each selected PSC to select PS pixels based on combination of both amplitude dispersion index and temporal coherence. Moreover, the PS pixels that appear to be persistent only in certain interferograms and those that appear to be dominated by scatterers in adjacent PS pixels may be discarded.

Although the sampling density of the selected PS points are high, the contribution of the phase difference between neighbouring PS pixels can still be greater than π due to the spatially uncorrelated component of look angle error. The error and master contribution on the look angle error have been estimated previously. Thus, these two terms are subtracted before phase unwrapping.

The phase values can then be unwrapped in three dimensions (i.e., two spatial and one temporal). Initially for the unwrapping process, we have to estimate the temporal phase differences in each PS that is selected. The spatial unwrapping can then be performed for each time step of a reference PS using an iterative approach. After that, unwrapped phase time series for each PS will then be integrated in time [7]. For correct phase unwrapping of a PS, the deformation between PS and at least one neighbouring PS in time or space must be less than half of the radar wavelength.

The unwrapped phase still contains the spatially correlated components of look angle error, atmospheric and orbital error which mask the deformation signal. These spatially correlated components are assumed to be uncorrelated temporally. Hence, the spatially correlated errors are estimated by high pass filtering the unwrapped data in time and then low pass filtering in space. Finally, subtracting the spatially correlated errors leave phase due to deformation, residual of spatially uncorrelated components

and unwrapping error components that can be modelled as noise. All the remaining phase noises are expected to be significantly reduced. Detailed descriptions of the StaMPS method can be found in [7] and [5].

III. RESULTS AND DISCUSSIONS

The spatially correlated errors due to look angle error (see Fig. 3), atmospheric and orbital errors for master (see Fig. 4) and atmospheric and orbital errors for slave images (see Fig. 5) are estimated and removed in order to obtain the interested parameter of deformation measurement.

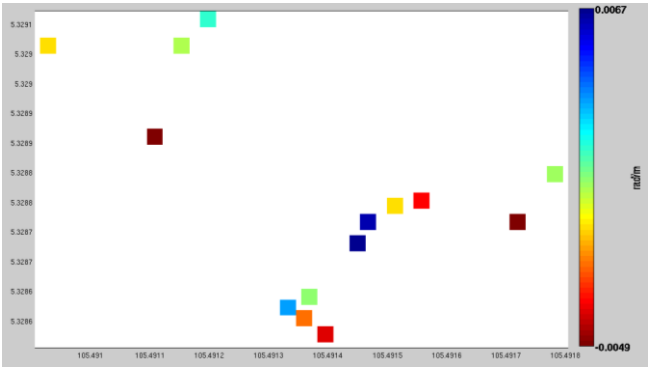

Fig. 3. Phase due spatially correlated look angle error in rad/meter.

Fig. 4. Phase due to master atmospheric and orbital errors.

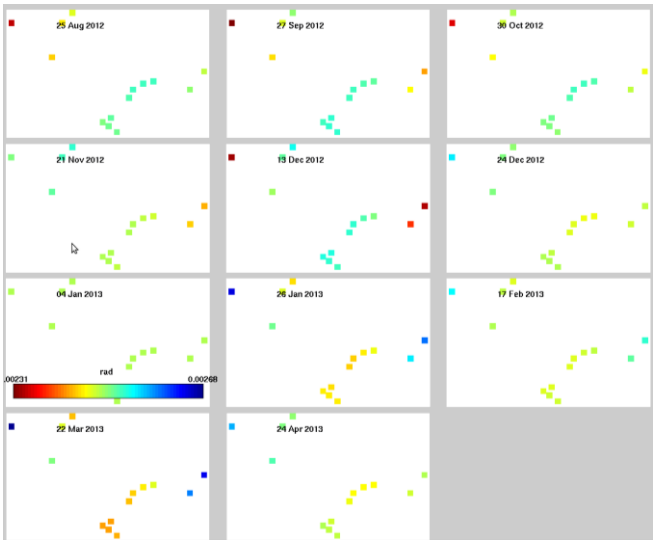

Fig. 5. Phase due to atmospheric and orbital errors in slave images.

A total number of 14 PS points are identified on the P platform using the StaMPS method (see Fig. 6). The colour levels of the PS points correspond to the variation of average deformation rates in the LOS direction which is from -6 mm/year (red) to 8.1 mm/year (blue). Two difference areas of the distribution PS points can be distinguished: the right side of the helipad area and the left side of the gas compression area. The number of PS points is higher in helipad area than gas compression area. However, no deformation measurements or PS points can be obtained in the middle of P platform and on the offshore support vessel (OSV). This is due to the middle portions of P platform and OSV have different object or scattering properties over different times, which cause temporal de-correlation effects, leading to a loss of coherence.

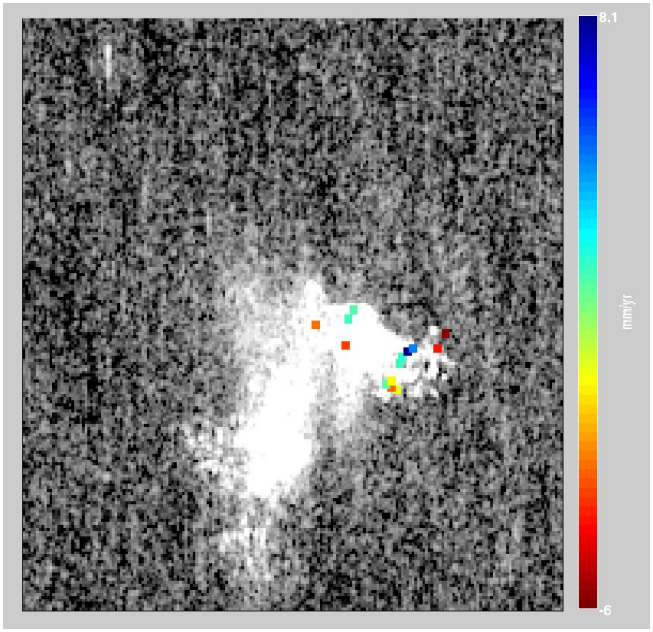

Fig. 6. The average LOS deformation rates in mm/yr for the 14 PS points are overlapped on the mean amplitude SAR image.

Fig. 7 shows that seven of the PS points are detected in the P platform have subsidence (i.e., range from -1 mm/year to -6 mm/year). On the contrary, another seven PS points demonstrates that uplift have occurred in the P platform (i.e., range from 1 mm/year to 8 mm/year). Thus, the subsidence and uplift rates of the P platform indicate that the P platform has small movement up and down. Fig. 8 shows the standard deviation of the estimated deformation rate which is from 0.8 to 3.1 mm/year. It is observed that the standard deviation values for the estimated deformation rate are small which implies the results are accurate and reliable.

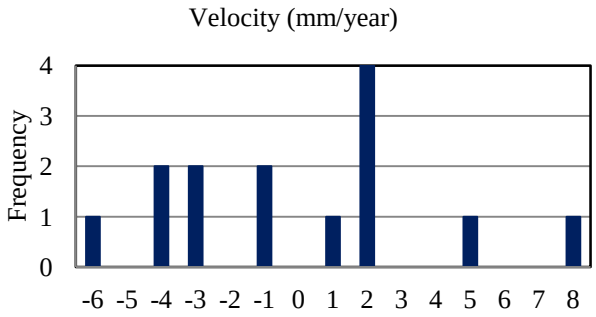

Fig. 7. Histogram representing the number of estimated deformation rate over the P platform.

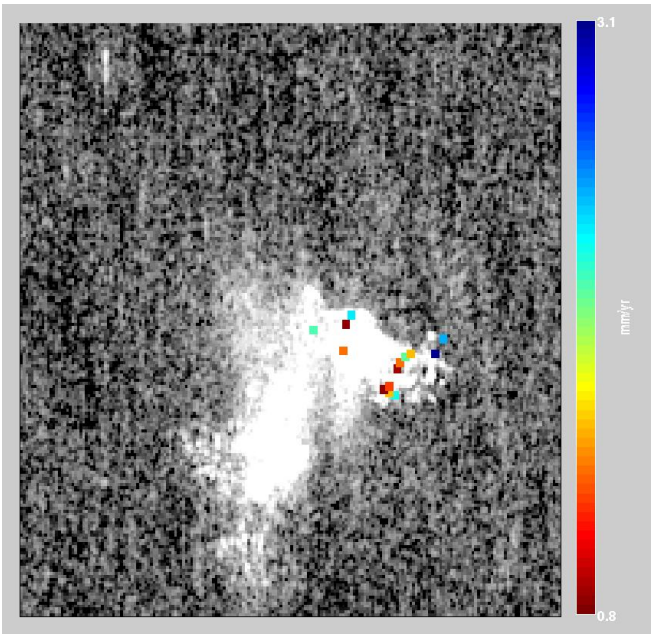

Fig. 8. Standard deviation of the estimated deformation rate.

Meanwhile, Fig. 9 shows the deformation time series of 14 PS points. The top subplot shows the perpendicular baseline in meters for each interferogram. In the main subplot, the time series of deformation is plotted. In the right subplot, the dates of interferograms are listed. The result in the main subplot show that the P platform experienced with the small deformation and nonlinear surface motions.

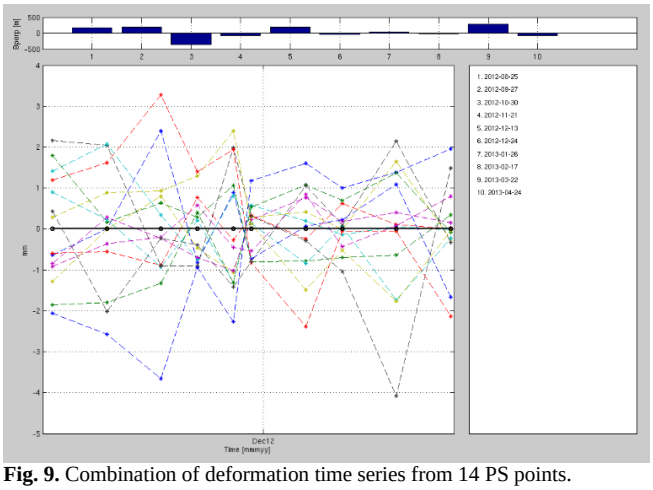

Fig. 9. Combination of deformation time series from 14 PS points.

IV. CONCLUSION

The deformation of P platform has been studied using the StaMPS method. 14 PS points are identified on the P platform. The PS points are able to extract the spatial and temporal information of the P platform deformation. This study has revealed that the P platform has experienced with the maximum subsidence and uplift rates of -6 mm/year and 8.1 mm/year, respectively. The small standard deviation values of the estimated deformation which range from 0.8 to 3.1 mm/year indicate the results are accurate and reliable. Analysis of the time series show the P platform experienced with the small deformation and nonlinear surface motions. In the next phase of this study, the number of SAR images will be increased to at least 25 images with long period of time in order to better understand the deformation of offshore platform monitored. The deformation results obtained from the StaMPS method will also be validated with the GPS technique.

REFERENCES

[1] Ferretti, A., C. Prati, and F. Rocca (2000). Nonlinear subsidence rate estimation using permanent scatterers in differential SAR interferometry. IEEE Transactions on Geoscience and Remote Sensing 38(5), 2202–2212.

[2] Hooper, A., H. Zebker, P. Segall, and B. Kampes (2004). A new method for measuring deformation on volcanoes and other non-urban areas using InSAR persistent scatterers. Geophysical Research Letters 31, L23611, doi:10.1029/2004GL021737.

[3] Widjajanti, N. and Matori A.N. (2009). Evaluation of GPS data for offshore platform subsidence, 7th Asia Pacific Structural Eng. And Construction Conf. (APSEC 2009) & 2nd European Asian Civ. Eng. Forum (EACEF2009), Langkawi, Malaysia.

[4] Matori, A. N., Amir, S. A. L., Harahap, I. S. H., and Perissin, D. (2014). Deformation Monitoring of Offshore Platform Using the Persistent Scatterer Interferometry Technique. Applied Mechanics and Materials. Vol. 567 (2014) pp 325-330.

[5] Sousa, J.J. (2009). Potential of Integrating PSI Methodologies in the Detection of Surface Deformation. PhD Thesis, University of Porto, Portugal.

[6] Ferretti, A., C. Prati, and F. Rocca (2001). Permanent scatterers in SAR interferometry. IEEE Transactions on Geoscience and Remote Sensing 39(1), 8–20.

[7] Hooper, A. (2006). Persistent Scatterer Radar Interferometry for Crustal Deformation Studies and Modeling of Volcanic Deformation. Ph. D. thesis, Stanford University.